Light Metals 2015
Edited by: Margaret Hyland
TMS (The Minerals, Metals & Materials Society), 2015

EFFECTS OF Zr AND V MICRO-ALLOYING ON ACTIVATION ENERGY DURING HOT DEFORMATION OF 7150 ALUMINUM ALLOYS

Cangji Shi, X.-Grant Chen
Department of Applied Science, University of Québec at Chicoutimi;
555 Boulevard Université; Saguenay, QC, G7H 2B1, Canada

Keywords: 7150 aluminum alloy, Zr addition, V addition, Hot compression, Constitutive analysis, Activation energy.

Abstract

The hot deformation behavior of 7150 aluminum alloys micro-alloyed with 0.12% Zr and 0.11% V was investigated using uniaxial compression tests conducted at various temperatures and strain rates. The results show that the flow stress levels increase significantly due to the additions of 0.12% Zr and 0.11% V. The activation energy for hot deformation has generally been treated as a constant value for a given material in literature. Using revised Sellars' constitutive analyses, the activation energy of a material is considered as a function of deformation temperature and strain rate. It is found that the activation energies of all three 7150 alloys decrease with increasing deformation temperature and increasing strain rate. The activation energies of the alloy containing 0.12% Zr are remarkably increased compared with the base alloy at most deformation conditions studied. The 0.11% V addition generally increases activation energies at the majority of deformation conditions, except at low temperatures and at low strain rates. Comparing the activation energy maps over all the deformation conditions applied for three alloys, the effects of micro-alloying of Zr and V on the plastic deformation under specific deformation conditions can be better understood.

Introduction

The 7xxx series aluminum alloys are very attractive materials to be used in the automotive and aerospace industries, due to a high strength-to-density ratio and excellent mechanical fracture toughness [1]. These aluminum alloys are generally subjected to hot forming processes such as rolling, forging and extrusion. The mechanical properties are influenced by the alloying elements and thermomechanical parameters, such as deformation temperature, strain rate and strain [2]. A clear understanding of the effects of micro-alloying and thermomechanical processing on the high temperature deformation behaviors is important to improve the mechanical properties of products.

The addition of zirconium is well known to increase the recrystallization resistance of aluminum alloys by forming fine, coherent Al_3Zr dispersoids [3]. The presence of the Al_3Zr dispersoids promotes the formation of a stable and refined subgrain structure during the hot working, which promotes additional substructure strengthening [4]. Vanadium addition is reported to maintain high temperature strength of the aluminum alloy by forming thermally stable dispersoids of $Al_{11}V$ [5]. The $Al_{11}V$ dispersoids could retard dynamic softening and raise recrystallization temperature during hot working processes [6].

Various constitutive models have been established to describe the flow stress behavior, including physical-based, phenomenological and artificial neural network models and equations [7]. Among all, the hyperbolic-sine law, proposed by Sellars and McTegart [8], has been proven to be most applicable over a wide range of stresses. The activation energy of a material for hot deformation derived from this relation is usually used as an indicator of the degree of difficulty of the hot deformation process. In the majority of research [7-10], the activation energy has been treated as a constant value for all applied hot deformation conditions. However, the activation energy for hot deformation represents the free energy barrier to dislocation slipping, which is affected by the temperature, external stress and microstructure during hot-forming processes [2]. A revised Sellars' constitutive equation has been proposed by our previous work [11], which considered the effects of deformation temperature and strain rate on the activation energy and material variables. However, under different deformation conditions, the effects of alloying elements on the evolution of activation energy for hot deformation of aluminum alloys have rarely been reported.

In the present paper, the hot deformation behavior of 7150 alloys with 0.12% Zr and 0.11% V additions is studied using hot compression tests performed at various temperatures and strain rates. The effects of Zr and V additions on the evolution of the activation energy of 7150 alloys using a revised Sellars' constitutive equation for different deformation conditions are investigated.

Experimental

Experiments were conducted on 7150 base alloy (Zr free) and alloys containing 0.12% Zr and 0.11% V respectively (all alloy compositions are in wt% unless otherwise indicated). The chemical compositions of those alloys are provided in Table I. Approximately 3 kg of each material was melted in an electrical resistance furnace and then cast into a rectangular permanent steel mold measuring 30 x 40 x 80 mm^3. The cast ingots of these alloys were homogenized at 465 °C for 24 h, followed by direct water quenching to room temperature. Cylindrical samples measuring 10 mm in diameter and 15 mm long were machined from the homogenized ingots. Uniaxial compression tests were conducted on a Gleeble 3800 thermomechanical simulation unit at strain rates of 0.001, 0.01, 0.1, 1 and 10 s^{-1} and deformation temperatures of 573, 623, 673 and 723 K, respectively. The samples were deformed to a total true strain of 0.8 and then immediately water-quenched to retain the microstructure at the deformation temperature. Some deformed samples were selected for electron backscattered diffraction (EBSD) analysis under a scanning electron microscope (SEM, JEOL JSM-6480LV). The step size between the scanning points was set to 1.0 μm.

Table I. Chemical composition of the alloys studied (wt%).

Alloy	Zn	Mg	Cu	Si	Fe	Zr	V	Al
7150 base alloy	6.44	2.47	2.29	0.16	0.15	-	0.01	Bal.
With 0.12%Zr	6.35	2.22	2.34	0.16	0.15	**0.12**	0.01	Bal.
With 0.11%V	6.31	2.30	2.24	0.16	0.14	-	**0.11**	Bal.

Results

Flow stress behavior

Typical true stress-true strain curves obtained during hot compression of the 7150 base alloy and the alloys with 0.12% Zr and 0.11% V are presented in Fig. 1. In general, the flow stress increases rapidly at the beginning of deformation and then either remains fairly constant or decreased to some extent after attaining a peak stress. For the three alloys, it is evident that the flow stress levels decrease with increasing deformation temperature and with decreasing strain rate. These observations are in good agreement with earlier reports on 7xxx alloys [2]. However, at the same deformation conditions, the flow stress values are improved significantly when being alloyed with 0.12% Zr and 0.11% V. It is observed that the alloy containing 0.11% V results in slightly higher values of flow stress compared with the same level of Zr addition (0.12%) at any given deformation condition. For example, at 573 K and with a strain rate of 1 s^{-1}, the alloys containing 0.12% Zr and 0.11% V display 6.2% and 7.9% increases in the peak flow stress relative to the base alloy respectively. At a higher temperature of 673 K and with a lower strain rate of 0.01 s^{-1}, the peak flow stresses increase by 7.3% and 13.4% due to the additions of Zr and V. Therefore, the addition of Zr and V could remarkably enhance the deformation resistance of the 7150 base alloy during hot deformation process. More detailed information about the evolution of flow stress in Zr and V microalloyed 7150 alloys can be found in [9,10].

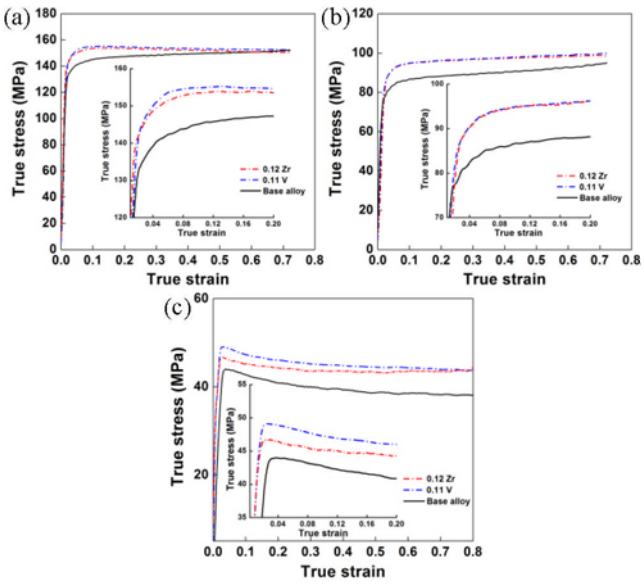

Figure 1. Typical true stress-true strain curves of 7150 base alloy and alloys containing 0.12% Zr and 0.11% V under deformation conditions at (a) T=573 °C and $\dot{\varepsilon}$ =1 s^{-1}; (b) T=673 °C and $\dot{\varepsilon}$ =1 s^{-1} and (c) T=673 °C and $\dot{\varepsilon}$ =0.01 s^{-1}.

Microstructure evolution

The initial microstructure of the 7150 base alloy and the alloys with 0.12% Zr and 0.11% V additions after homogenization has been reported in our previous studies [9,10]. The homogenized structures of the three alloys were composed of uniform equiaxed grains formed during casting. The precipitation of a relatively large number of coherent Al_3Zr dispersoids with an average diameter of 15 nm was observed in the alloy containing 0.12% Zr. When 0.11% V was added, a remarkable amount of $Al_{21}V_2$-type dispersoids with an average diameter of 51 nm were precipitated in the microstructure.

To investigate the microstructural evolution during the hot compression process, orientation imaging maps were generated under different deformation conditions using the EBSD technique, as shown in Fig. 2. In EBSD analysis, the boundary misorientation angles can be distinguished as follows: white lines: 1-5°; blue lines: 5-15°; thin black lines: 15-30° and thick black lines: (> 30°).

Under the deformation condition at 573 K and 1 s^{-1}, the original grains of the three alloys were severely torn and broke into irregular deformation bands (Fig. 2a, b and c). A large number of low-angle boundaries of 1-5° are observed inside the elongated grains, indicating a high density of cell and subgrain structures. As the temperature increases to 673 K and the strain rate decreases to 0.1 s^{-1}, the deformation of all three alloys becomes more homogeneous, and the recovered substructures become better organized with larger subgrains (Fig. 2d, e and f). In the base alloy, a large number of subgrains with higher angle boundaries (5-15°) exist along the serrated grain boundaries (Fig. 2d), indicating a strong dynamically recovered structure. However, the recovered substructures in the alloys containing 0.12% Zr and 0.11% V are mainly characterized by low-angle boundaries of 1-5° (Fig. 2e and f). This suggests a restrained level of dynamic recovery with the additions of Zr and V due to the pinning effects of Al_3Zr and $Al_{21}V_2$ dispersoids on dislocation motion and subgrain coalescence [9, 10], thereby resulting in significant increases in the flow stress.

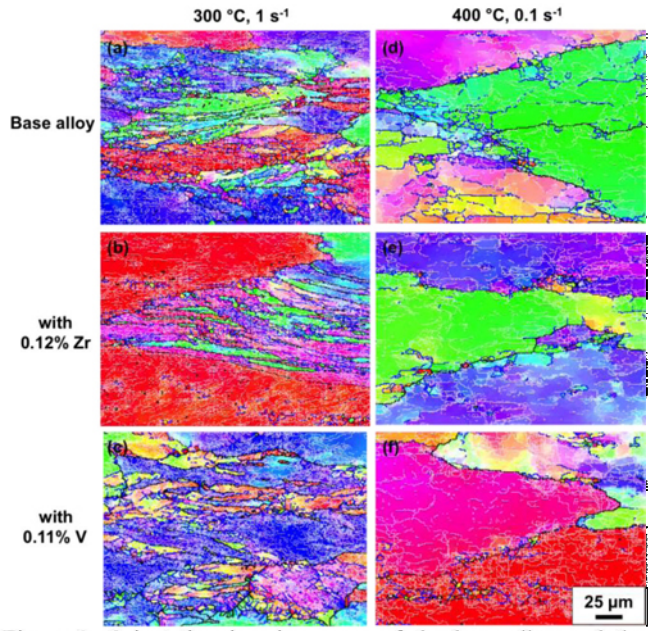

Figure 2. Orientation imaging maps of the base alloy and the alloys with 0.12% Zr and 0.11% V under different deformation conditions.

Evolution of activation energy during hot deformation

The hyperbolic-sine equation, proposed by Sellars and McTegart [8], has been widely used to model the hot deformation behavior of the materials over a wide range of stresses, as given in Eq. (1).

$$\dot{\varepsilon} = A[\sinh(\alpha\sigma_p)]^n \exp(-\frac{Q}{RT}) \quad (1)$$

where, n and A are material constants, α is the stress multiplier, σ_p is the peak flow stress (MPa), Q is the activation energy for hot deformation (kJ/mol), R is the universal gas constant (8.314 J/mol K), and T is the deformation temperature (K).

The activation energy for hot deformation, Q derived from Eq. (1) is an important physical parameter serving as an indicator of the degree of difficulty of plasticity deformation. In the original Sellars' equation, n , A and the activation energy Q are considered to be material constants which are independent of the deformation conditions (T and $\dot{\varepsilon}$).

Using the original Sellars' equation and experimental data obtained from the true stress-true stain curves at different deformation conditions, the activation energies, Q for three alloys were calculated [9,10] and listed in Table II. By comparison of activation energy values of three materials, we can only get a general conclusion, namely that the micro-alloying of Zr and V considerably increases the difficulty of plasticity deformation of the 7150 alloy.

Table II. Activation energy, Q calculated by the original Sellars' equation and experimental flow stress data (kJ/mol).

Alloy	7150 base alloy	With 0.12%Zr	With 0.11%V
Q	229	247	242

In fact, the values of n and A were observed to vary with the deformation temperature or strain rate in our pervious studies [9-11] and other studies [7, 8]. Moreover, the hot deformation of aluminum alloys occurs mainly by dislocation slipping, which is a thermally activated process [2]. The activation energy of dislocation slip is reduced by applied external stress, and the deformation difficulty is affected by temperature [2]. It is obvious that hot deformation process involves dislocation slip, and the effects of thermomechanical factors on the evolution of the activation energy should be considered. Therefore, the original Sellars' equation (Eq. 1) cannot adequately represent the hot deformation behavior of aluminum alloys.

To overcome the shortcomings of the original Sellars' equation, a revised Sellars' constitutive analysis has been proposed in our previous study [11] and is given in Eq. (2). Eq. (2) considers the effects of the deformation temperature and strain rate on the material variables and activation energy, which has been proven to provide an accurate estimate of flow stress behavior of the 7150 aluminum alloy. In the present study, to investigate the effects of micro-alloying of Zr and V on the activation energy under different deformation conditions, three alloys including the base alloy (Table I) were selected and the evolution of activation energy is evaluated based on Eq. (2).

$$\dot{\varepsilon} = A(T,\dot{\varepsilon})[\sinh(\alpha\sigma_p)]^{n(T)} \exp(-\frac{Q(T,\dot{\varepsilon})}{RT}) \quad (2)$$

where, the material variables n , A and activation energy Q are functions of the deformation temperature and the strain rate.

The experimental data obtained for the 7150 base alloy are used as an example to derive the values of activation energy Q under different deformation conditions for all materials studied. The data obtained at a strain rate of 10 s^{-1} were not taken into account due to the flow instability leading to a significant rise in deformation temperature [9, 10]. The stress multiplier α can be defined as $\alpha = \beta / n_1$ [8], where β and n_1 are evaluated from the slopes of the plots of $\ln(\dot{\varepsilon})$ - σ_p and $\ln(\dot{\varepsilon})$ - $\ln(\sigma_p)$, respectively, for the range of temperatures studied. Hence, the value of α for the base alloy is determined to be 0.011.

Taking the natural logarithm of both sides of Eq. (2) yields [11],

$$\ln\dot{\varepsilon} = [\ln A(T,\dot{\varepsilon}) - \frac{Q(T,\dot{\varepsilon})}{RT}] + n(T)\ln[\sinh(\alpha\sigma_p)] \quad (3)$$

The values of n at each deformation temperature can be obtained from the slopes of the $\ln\dot{\varepsilon}$ - $\ln[\sinh(\alpha\sigma_p)]$ plots (Fig. 3a). By linear fitting, a good linear relationship between n and the deformation temperature is obtained (Fig. 3b), which is expressed in Eq. (4). The regression coefficients are presented in Table III. It is evident that the n value decreases linearly with increasing temperature.

$$n = B_0 + B_1 T \quad (4)$$

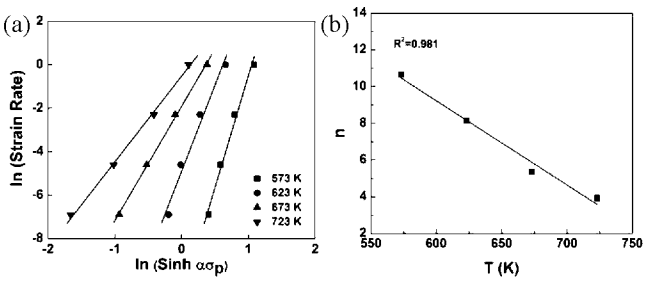

Figure 3. Relationships between (a) $\ln\dot{\varepsilon}$ and $\ln[\sinh(\alpha\sigma_p)]$ and (b) n and T of the 7150 base alloy.

At a constant strain rate, partial differentiation of Eq. (2) yields [11],

$$Q(T,\dot{\varepsilon}) = Rn(T)[\frac{\partial \ln[\sinh(\alpha\sigma_p)]}{\partial(1/T)}]_{\dot{\varepsilon}} = Rn(T)S(\dot{\varepsilon}) \quad (5)$$

Based on the measured true stress-true strain data, the values of S at each of the strain rates can be determined from the slopes of the $\ln[\sinh(\alpha\sigma_p)]$ - $1/T$ plots (Fig. 4a). From regression fitting, an excellent polynomial relationship between S and strain rate is found (Fig. 4b), as expressed in Eq. (6). The regression coefficients in Eq. (6) for all three alloys studied are listed in Table III. Based on the obtained $n(T)$ and $S(\dot{\varepsilon})$ functions, the activation energy $Q(T,\dot{\varepsilon})$ can be calculated in Eq. (7).

$$S = C_0 + C_1(\ln\dot{\varepsilon}) + C_2(\ln\dot{\varepsilon})^2 \quad (6)$$

$$Q = R[B_0C_0 + C_0B_1T + B_1C_1T(\ln\dot{\varepsilon}) + B_1C_2T(\ln\dot{\varepsilon})^2 + B_0C_1(\ln\dot{\varepsilon}) + B_0C_2(\ln\dot{\varepsilon})^2] \quad (7)$$

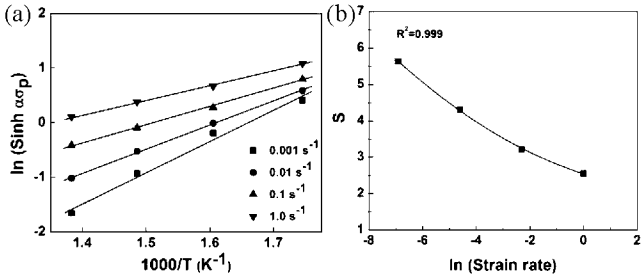

Figure 4. Relationships between (a) $\ln[\sinh(\alpha\sigma_p)]$ and $1000/T$ and (b) S and $\ln\dot{\varepsilon}$ of the 7150 base alloy.

Table III. Regression Coefficients in Eq. (4) and (6) for all three alloys studied.

Alloy	Coefficients				
	B_0	B_1	C_0	C_1	C_2
7150 base alloy	36.76	-0.046	2.54	-0.233	0.031
With 0.12%Zr	38.69	-0.048	2.74	-0.088	0.050
With 0.11%V	33.02	-0.040	2.93	-0.286	0.009

Fig. 5a illustrates the evolution of Q values of the base alloy calculated from the experimental data by substituting the values of n at each deformation temperature and S at each strain rate into Eq. (5). The predicted Q values – activation energy map of the base alloy - derived from Eq. (7) are shown in Fig. 5b, which demonstrate excellent agreement with those obtained from the experimental data (Fig. 5a). It is evident that the activation energy for hot deformation decreases with increasing temperature and strain rate, where it reaches 500 kJ/mol at 573 K and 0.001 s^{-1}, whereas declines by 83% (84 kJ/mol) at 723 K and 1 s^{-1}, indicating decreasing deformation difficulty as the temperature and the strain rate increase. The results in Fig. 5a and b reveal that the activation energy for hot deformation cannot be treated solely by a constant value, but varies over a wide range of temperature and strain rate.

Likewise, the material variables n and S for the alloys containing 0.12% Zr and 0.11% V are calculated according to Eq. (2), (3) and (5), and display excellent linear relationships with T and polynomial relationships with $\dot{\varepsilon}$ respectively. Consequently, the activation energy maps of the alloys with 0.12% Zr and 0.11% V are predicted according to Eq. (7), as illustrated in Fig. 5c and d. Furthermore, in an attempt to gain more insight into the effects of micro-alloying of Zr and V on the activation energy at various working conditions, the variations in activation energy values under different deformation temperatures and strain rates are illustrated in Fig. 6.

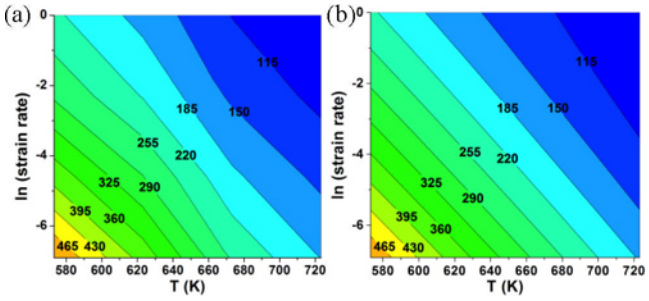

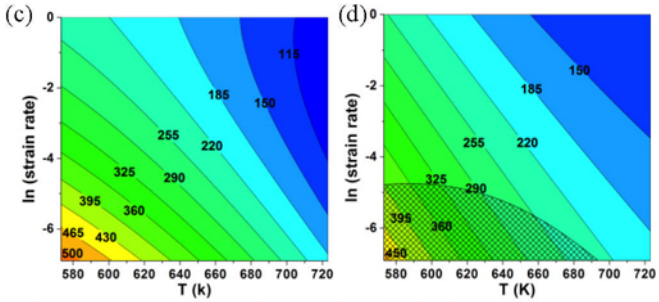

Figure 5. Evolution of Q value (kJ/mol) as a function of deformation temperature and strain rate: (a) experimental results and (b) predicted results of the 7150 base alloy; and predicted results of the alloys with (c) 0.12% Zr and (d) 0.11% V.

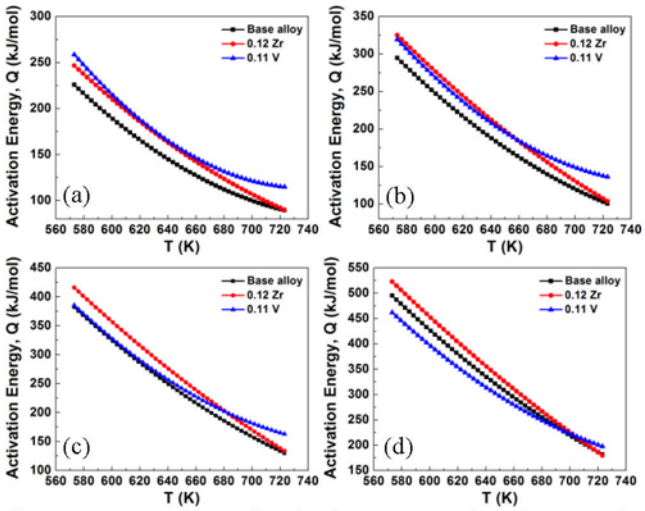

Figure 6. Comparison of activation energy values between the 7150 base alloy and alloys with 0.12% Zr and 0.11% V as a function of deformation temperature at the strain rates of (a) 1 s^{-1}; (b) 0.1 s^{-1}; (c) 0.01 s^{-1}; and (d) 0.001 s^{-1}.

Discussion

In general, the activation energies for hot deformation of all 7150 alloys are quite sensitive to the deformation conditions, and decrease with increasing deformation temperature and strain rate, indicating that plastic deformation occurs more easily as the temperature and strain rate increase (Fig. 5). This is closely correlated with the thermodynamic mechanism of dislocation movement. It is understood that thermal activation, which favors overcoming the energy barrier to dislocation motion, increases with increasing temperature [12]. In addition, the level of dynamic recovery is improved with increasing temperature, and the dislocation density is reduced to facilitate further dislocation motion [2]. Hence, the increasing temperature could substantially reduce the resistance to dislocation slipping and decrease the activation energy for hot deformation.

On the other hand, the applied external force increases with increasing strain rate and leads to an augmented shear stress to activate the motion of dislocations [12]. Besides, the dislocation multiplication rate increases with increasing strain rate, thereby resulting in an increase in the rate of dynamic recovery [2]. Thus, the increasing strain rate results in an increased shear stress and a higher rate of dynamic recovery, attributing to the decrease in activation energy.

When the material is alloyed with 0.12% Zr, the levels of activation energy generally increase at most deformation conditions compared to the base alloy (Fig. 5b and c). For example, under the deformation condition at 573 K and 0.001 s^{-1}, the activation energy of the base alloy is 500 kJ/mol, which increases to 520 kJ/mol due to the 0.12% Zr addition. As the deformation temperature increases to 673 K and the strain rate increases to 1 s^{-1}, the activation energy of the alloy containing 0.12% Zr increased to 137 kJ/mol, representing 21.4% increase relative to that of the base alloy.

Moreover, it is observed from Fig. 6 that, at all constant strain rates, the increments in activation energy at lower deformation temperatures are remarkably higher than those at higher deformation temperatures due to the Zr addition. Towards 723 K, the values of activation energy of both alloys (base and 0.12%Zr) are getting much closer. These results indicate that micro-alloying with 0.12% Zr increases the deformation resistance during hot deformation preferentially at low deformation temperatures.

The addition of 0.11% V also generally increases activation energies under the majority of deformation conditions compared to the base alloy. However, the activation energies are observed lower than those of the base alloy, when the deformation is performed at lower deformation temperatures (573-700 K) and at low strain rates (0.001 and 0.008 s^{-1}), as indicated by the shadow region in Fig. 5d, which suggests easier conduction of deformation under those conditions with V-contained alloy.

Moreover, Fig. 6c reveals that at a low stain rate of 0.01 s^{-1}, the values of activation energy of the 0.11%V alloy are almost the same as the base alloy at lower deformation temperatures (573-630 K). It is even more evident in Fig. 6d that at the lowest stain rate of 0.001 s^{-1}, the activation energies are much lower than those of the base alloy at such low deformation temperatures. Hence, during hot deformation at low temperatures and low strain rates, the 0.11%V alloy may show a similar or a better hot workability than the base alloy. The mechanism behind will be a subject of future investigation.

The present study demonstrates that the activation energy map for hot deformation can not only describe the thermomechanical dependency of the activation energy for each material, but also reveal more valuable technical details on the hot workability under various deformation conditions, which could not be addressed solely based on a constant value of the activation energy for a given material. By comparing the activation energy maps over all deformation conditions applied for three alloys, the effects of microalloying of Zr and V on the plastic deformation of 7150 alloys under specific deformation conditions are better discovered. Therefore, the activation energy map may provide a powerful tool for optimizing the hot working process of metals and alloys.

Conclusions

1. With the additions of 0.12% Zr and 0.11% V, the flow stresses of 7150 alloys increase significantly due to the retardation of dynamic recovery induced by the pinning effects of Al_3Zr and $Al_{21}V_2$ dispersoids on dislocation motion and subgrain coalescence.
2. Using a revised Sellars' constitutive equation, the activation energy maps for hot deformation of 7150 alloys are proposed, which are considered as a function of deformation temperature, strain rate and micro-alloying elements.
3. The activation energies for hot deformation of the alloy with 0.12% Zr are remarkably increased compared to those of the base alloy at most deformation conditions. The Zr-contained alloy increases the deformation resistance during hot deformation preferentially at low deformation temperatures.
4. The 0.11% V addition generally increases activation energies at the majority of deformation conditions, except at low deformation temperatures (573-700 K) and at low strain rates (0.001 and 0.008 s^{-1}), where reduced activation energies are found compared to the base alloy.

Acknowledgments

The authors would like to acknowledge the financial support from the Natural Sciences and Engineering Research Council of Canada (NSERC) and from Rio Tinto Alcan through the NSERC Industrial Research Chair in Metallurgy of Aluminum Transformation at the University of Québec at Chicoutimi. The authors would also like to thank Ms. E. Brideau for her assistance in the hot compression tests performed on the Gleeble 3800 thermomechanical simulator.

References

[1] E.A. Starke and J.T. Staley, "Application of modern aluminum alloys to aircraft," *Progress in Aerospace Sciences*, 32 (1996), 131-172.

[2] H.J. McQueen, S. Spigarelli, M. Kassner, E. Evangelista, *Hot Deformation and Processing of Aluminum Alloys*, CRC Press, Florida, 2011, pp. 87-233.

[3] J.D. Robson, "A new model for prediction of dispersoid precipitation in aluminium alloys containing zirconium and scandium," *Acta Materialia*, 52 (2004), 1409-1421.

[4] Y.V. Milman et al., "Microstructure and mechanical properties of cast and wrought Al-Zn-Mg-Cu alloys modified with Zr and Sc," *Materials Science Forum*, 396-402 (2002), 1217-1222.

[5] K.E. Knipling, D.C. Dunand and D.N. Seidman, "Criteria for developing castable, creep-resistant aluminum-based alloys-A review," *Zeitschrift für Metallkunde*, 97 (2006), 246-265.

[6] J.R. Davis, *ASM Specialty Handbook: Aluminum and Aluminum Alloys*, (OH: American Society for Metals, Metals Park, 1993), 23-58.

[7] Y. Lin and X. Chen, "A critical review of experimental results and constitutive descriptions for metals and alloys in hot working," *Materials and Design*, 32 (2011), 1733-1759.

[8] C.M. Sellars and W.J. McTegart, "La relation entre la resistance et la structure dans la deformation a chaud," *Mémoires Scientifiques de la Revue de Metallurgie*, 63 (1966), 731-746.

[9] C. Shi and X.G. Chen, "Effect of Zr addition on hot deformation behavior and microstructural evolution of AA7150 aluminum alloy," *Materials Science and Engineering A*, 596 (2014), 183-193.

[10] C. Shi and X.G. Chen, "Effect of vanadium on hot deformation and microstructural evolution of 7150 aluminum alloy," *Materials Science and Engineerin A*, 613 (2014), 91-102.

[11] C. Shi, W. Mao and X.G. Chen, "Evolution of activation energy during hot deformation of AA7150 aluminum alloy," *Materials Science and Engineering: A*, 571 (2013), 83-91.

[12] D. Caillard and J.L. Martin, *Thermally Activated Mechanisms in Crystal Plasticity*, (Oxford: Pergamon Press, 2003), 1-280.